DALTON

# Synthesis, crystal structure and non-linear optical properties of two new cluster compounds, $[MoCu_3OS_3(PPh_3)_3\{S_2P(OBu)_2\}]$ and $[MoAg_3S_4(PPh_3)_3\{S_2P(OBu^i)_2\}]$

**De-liang Long,[a] Shu Shi,*[,a] Xin-quan Xin,*[,a] Bao-sheng Luo,[b] Liao-rong Chen,[b] Xiao-ying Huang[c] and Bei-sheng Kang[c]**

[a] *State Key Laboratory of Coordination Chemistry, Coordination Chemistry Institute, Nanjing University, Nanjing, 210093, China*
[b] *Analysis and Testing Center, Wuhan University, Wuhan, 430072, China*
[c] *State Key Laboratory of Structural Chemistry, Fujian Institute of Research on the Structure of Matter, Chinese Academy of Science, Fuzhou, Fujian, 350002, China*

Two novel O,O'-dialkyl dithiophosphate-containing Group 11–Group 16 sulfido clusters, $[MoCu_3OS_3(PPh_3)_3\{S_2P(OBu)_2\}]$ **1** and $[MoAg_3S_4(PPh_3)_3\{S_2P(OBu^i)_2\}]$ **2**, have been synthesised through reactions of $[NEt_4]_2[MoOS_3]$ with $Cu[S_2P(OBu)_2]$ and $[NEt_4]_2[MoS_4]$ with $Ag[S_2P(OBu^i)_2]$ respectively in dichloromethane and in the presence of $PPh_3$. The clusters crystallise in orthorhombic and triclinic forms respectively. The X-ray crystallographic structure determinations show that both clusters have a partial open cubane-like structure. The dithiophosphate ligands adopt a triply bridging role, employing two sulfur atoms to co-ordinate to the three Group 11 metal (M) atoms: one sulfur atom binds to one M atom, the other to two other M atoms. The clusters are soluble in common organic solvents and exhibit both non-linear absorption and non-linear refraction (self defocusing). Cluster **2** also exhibits a sizeable optical limiting effect.

Recent studies have revealed that many inorganic clusters exhibit very interesting non-linear optical (NLO) properties.[1,2] Unfortunately, direct technical applications are often frustrated by the cluster's low solubility in common organic solvents. One way to circumvent this practical problem is to introduce bulky organic ligands to the clusters to increase their solubility. *O,O'*-Di-*n*-butyl dithiophosphate and *O,O'*-diisobutyl dithiophosphate were selected for this purpose in the present study. Here we report the syntheses, crystal structures and non-linear optical properties of two sulfido clusters $[MoCu_3OS_3(PPh_3)_3\{S_2P(OBu)_2\}]$ **1** and $[MoAg_3S_4(PPh_3)_3\{S_2P(OBu^i)_2\}]$ **2**.

## Experimental

### Materials

All reagents and solvents were A.R. or C.P. grade used without further purification. The reagents $[NEt_4]_2[MoS_4]$ and $[NEt_4]_2[MoOS_3]$ were prepared according to the literature.[3]

### Preparations

**$Cu[S_2P(OBu)_2]$.** The compound $P_2S_5$ (4.4 g, 20 mmol) was dissolved in BuOH (25 $cm^3$) upon heating. The resultant solution was allowed to cool, then methanol (50 $cm^3$) and CuCl (3.0 g, 30 mmol) were added. The mixture was stirred for 50 h and then filtered. The white product was washed with methanol and recrystallised from dichloromethane (Found: C, 31.35; H, 6.05. Calc. for $C_8H_{18}CuO_2PS_2$: C, 31.50; H, 5.95%). IR (KBr pellets): ν(P–O) 1002.0, ν(P–S) 646.2 $cm^{-1}$.

**$Ag[S_2P(OBu^i)_2]$.** The compound $P_2S_5$ (4.4 g, 20 mmol) was dissolved in $Bu^iOH$ (25 $cm^3$) as above. To the resultant cold solution solid $Ag_2O$ (3.5 g, 15 mmol) was added. The mixture was stirred for 50 h and then filtered. The white precipitate was recrystallised from dichloromethane. Yield 4.2 g (Found: C, 27.90; H, 5.45. Calc. for $C_8H_{18}AgO_2PS_2$: C, 27.50; H, 5.20%). IR (KBr pellets): ν(P–O) 1007.0, ν(P–S) 646.3 $cm^{-1}$.

**$[MoCu_3OS_3(PPh_3)_3\{S_2P(OBu)_2\}]$ 1.** The compounds $Cu[S_2P(OBu)_2]$ (0.91 g, 3 mmol) and $PPh_3$ (0.79 g, 3 mmol) were dissolved in dichloromethane (40 $cm^3$) with stirring, then $[NEt_4]_2[MoOS_3]$ (0.44 g, 1 mmol) was added. The solid gradually dissolved and the solution became dark red. After stirring for 4 h the solution was filtered, the filtrate evaporated at room temperature affording a red oil and about 5 $cm^3$ clear solution. Discarding the solution, the oil was redissolved in dimethylformamide (5 $cm^3$), then layered with hexane (20 $cm^3$). Deep red crystals (0.8 g) were obtained several days later (Found: C, 51.95; H, 4.20. Calc. for $C_{62}H_{63}Cu_3MoO_3P_4S_5$: C, 52.20; H, 4.45%). IR (KBr pellets): ν(P–O) 998.5, ν(P–S) 635.2, 650.3, ν(Mo–O) 913.7 and ν(Mo–$S_b$) 444.5 $cm^{-1}$.

**$[MoAg_3S_4(PPh_3)_3\{S_2P(OBu^i)_2\}]$ 2.** The compounds $Ag[S_2P(OBu^i)_2]$ (1.05 g, 3 mmol) and $PPh_3$ (0.79 g, 3 mmol) were dissolved in dichloromethane (40 $cm^3$) with stirring. Solid $[NEt_4]_2[MoS_4]$ (0.44 g, 1 mmol) was added and dissolved gradually. After stirring for 4 h the dark red solution was filtered. The filtrate was layered with hexane (20 $cm^3$) and allowed to stand at room temperature for several days. Deep red crystals (0.9 g) were obtained (Found: C, 47.10; H, 4.20. Calc. for $C_{62}H_{63}Ag_3MoO_2P_4S_6$: C, 47.25; H, 4.05%). IR (KBr pellets): ν(P–O) 994.0, ν(P–S) 649.0, ν(Mo–$S_b$) 439.2, 418.2, ν(Mo–$S_t$) 495.0 $cm^{-1}$.

### Crystallography

The crystal data for compounds **1** and **2** are summarised in Table 1, together with some experimental details. Crystals of **1** with dimensions 0.40 × 0.35 × 0.25 mm and of **2** with dimensions 0.60 × 0.40 × 0.30 mm were mounted in random orientation on glass fibres. Diffraction data were collected on an Enraf-Nonius CAD4 diffractometer using graphite-monochromated Mo-Kα radiation (λ = 0.710 73 Å). Cell constants were obtained by least-squares fit to 25 diffraction maxima (for **1**, 9.45 < θ < 12.16; for **2**, 10.81 < θ < 14.72°). The intensities were not corrected but an absorption correction was applied

using empirical scan data. The structures were solved by direct methods. All non-H atoms were located in the *E* map. The structures were refined by full-matrix least-squares fits, initially with coordinates and isotropic thermal parameters, ultimately with coordinates and anisotropic thermal parameters of all non-H and non-C atoms for **1** and of all non-H atoms for **2**. The function minimised was $\Sigma w(|F_o| - |F_c|)^2$ and the weight $w$ was $1/\sigma^2(F)$. Hydrogen atoms were located geometrically and not refined. Calculations were performed on a PDP 11/44 computer using the MULTAN 82 program package[4] for **1** and a MicroVAX3100 computer using the TEXSAN program package[5] for **2**. The scattering factors for non-hydrogen elements were taken from Cromer and Waber.[6]

Atomic coordinates, thermal parameters and bond lengths and angles have been deposited at the Cambridge Crystallographic Data Centre (CCDC). See Instructions for Authors, *J. Chem. Soc., Dalton Trans.*, 1996, Issue 1. Any request to the CCDC for this material should quote the full literature citation and the reference number 186/78.

### Spectroscopic, NLO and other measurements

Elemental analyses were carried out on a Perkin-Elmer 240C elemental analyser. Infrared spectra were recorded on a Nicolet 170sx FT-IR spectrometer, UV/VIS spectra on a Shimaduz UV-240 spectrometer with dichloromethane as solvent.

For optical measurements dichloromethane solutions of compounds **1** and **2** were placed in a 1 mm quartz cuvette. The optical responses of the clusters were induced by linearly polarised, 7 ns pulses produced by a Q-switched frequency-doubled Nd:YAG laser. The spatial profiles of the optical pulses ($\lambda$ = 532 nm) were nearly Gaussian and the light was focused onto the sample with a mirror of 25 cm focal length. The radius of the laser beam waist was measured to be 30 μm (half-width at $1/e^2$ maximum). The interval between the laser pulses was set to be 10 s for operational convenience. The incident and transmitted pulse energies were measured coincidentally by two laser precision detectors (RjP-735 energy probes) communicating to a computer *via* an IEEE interface. An aperture of 2.5 cm diameter was positioned right in front of the transmission detector to capture the overall effect of both NLO absorption and NLO refraction on the optical limiting (OL) performance and Z-scan[7,8] results.

## Results and Discussion

### Synthesis

The synthetic routes to compounds **1** and **2** are designed based on the concept of unit construction. The $Cu[S_2P(OBu)_2]$ {or $Ag[S_2P(OBu^i)_2]$} unit was presynthesised and then treated with a mixture containing $PPh_3$ and $[MoOS_3]^{2-}$ (or $PPh_3$ and $[MoS_4]^{2-}$). It is known that a butterfly-shaped cluster $[MoCu_2OS_3(PPh_3)_3]$ can be isolated from a reaction mixture containing $Cu^+$, $PPh_3$ and $[MoOS_3]^{2-}$.[9a] As hypothesised in Scheme 1, when a butterfly-shaped unit encounters a $Cu[S_2P(OBu)_2]$ {or an $Ag[S_2P(OBu^i)_2]$ unit already existing in the solution} it is highly plausible that these two units will stabilise one another by formation of cluster **1** (or **2**).

The $[MoS_4]^{2-}$ moiety has a known tendency to pick up silver cations from solution to form linear $AgS_2MoS_2Ag$ or $MoS_4Ag_3$ fragments which in turn can polymerise into one-dimensional chains or two-dimensional sheets.[9b] The introduction of presynthesised $Ag[S_2P(OBu^i)_2]$ has apparently made the formation of discrete cluster **2** an energetically more favoured process than the polymerisation. It is interesting that all of the Cu atoms in **1** and Ag atoms in **2** adopt four-coordination. The chelating dithiophosphate ligands failed to replace the monodentate $PPh_3$. This is partially attributable to the small S–P–S chelating angle of the phosphate and to the strong bonds between the M′ and P atoms.

### Crystal structure

Clusters **1** and **2** are among the few known dithiophosphate-containing Group 11–Group 16 compounds.[10] The clusters are neutral and their structures resemble roughly that of cubane-like clusters, $[MoM'_3S_3Y(PPh_3)_3X]$ (Y = S or O; M′ = Cu or Ag; X = Cl, Br or I), with a dithiophosphate ligand occupying the position of X. The ORTEP diagrams of the clusters are shown in Figs. 1 and 2.

Of the two sulfur atoms in the dithiophosphate ligand, one binds to two M′ atoms (Cu in **1**, Ag in **2**) whereas the other binds to only one M′. While all of the three Cu–SP(S)$(OBu)_2$ and three Ag–SP(S)$(OBu^i)_2$ bond lengths (Tables 2 and 3) are within normal ranges,[12,13] those from the monodentate S atom

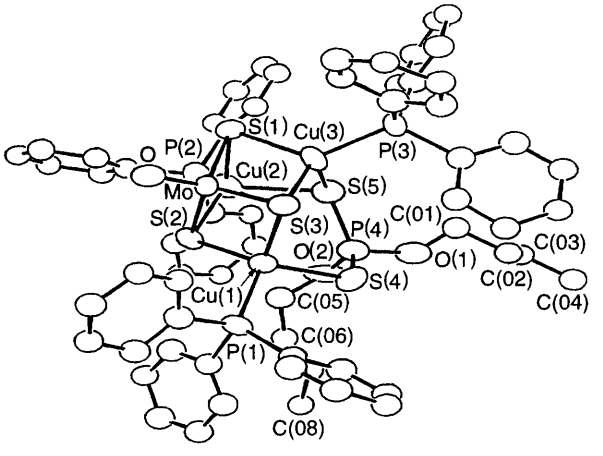


**Fig. 1** Crystal structure of $[MoCu_3OS_3(PPh_3)_3\{S_2P(OBu)_2\}]$ **1**. Labelling of phenyl carbon atoms is omitted for clarity

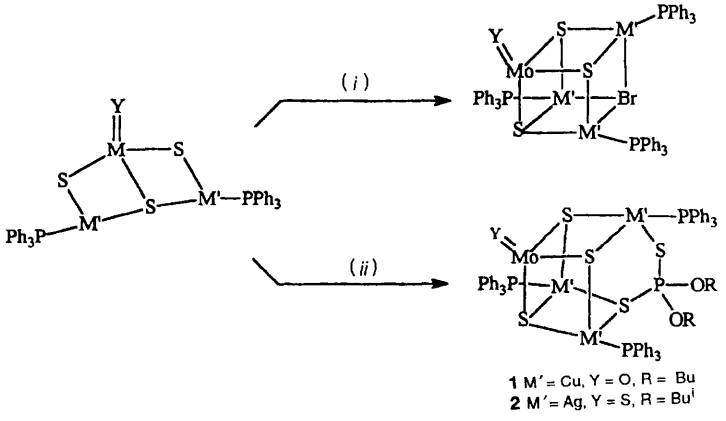


**Scheme 1** (*i*) $[M'Br(PPh_3)]$; (*ii*) $[M'(PPh_3)\{S_2P(OR)_2\}]$

**Table 1** Crystallographic data for compounds **1** and **2**

| | **1** | **2** |
|---|---|---|
| Chemical formula | $C_{62}H_{63}Cu_3MoO_3P_4S_5$ | $C_{62}H_{63}Ag_3MoO_2P_4S_6$ |
| Formula weight | 1426.97 | 1575.98 |
| Crystal system | Orthorhombic | Triclinic |
| Space group | $P2_12_12_1$ | $P\bar{1}$ |
| $a$/Å | 12.756(5) | 11.859(6) |
| $b$/Å | 13.571(2) | 14.554(8) |
| $c$/Å | 37.039(9) | 20.328(7) |
| $\alpha$/° | | 86.97(4) |
| $\beta$/° | | 99.84(4) |
| $\gamma$/° | | 108.23(5) |
| $U$/Å$^3$ | 6411.8(7) | 3283(6) |
| $Z$ | 4 | 2 |
| $\mu$/cm$^{-1}$ | 14.678 | 13.75 |
| $F(000)$ | 2912 | 1580 |
| $2\theta$/° | 50.0 | 50.0 |
| $hkl$ Ranges | 0–15, 0–16, 0–44 | 0–14, −17 to 17, −24 to 24 |
| $D_c$/g cm$^3$ | 1.478 | 1.59 |
| $T$/K | 293 | 296 |
| Residuals: $R$, $R'$ | 0.056, 0.065 | 0.050, 0.064 |
| No. unique data | 6273 | 11 521 |
| No. observed [$I > 3\sigma(I)$] | 3301 | 9871 |
| No. variables | 393 | 703 |
| Maximum shift in final cycle | 0.16 | 0.05 |
| Largest peaks in final difference map/e Å$^{-3}$ | 0.83, 0.42 | 0.79, −1.44 |

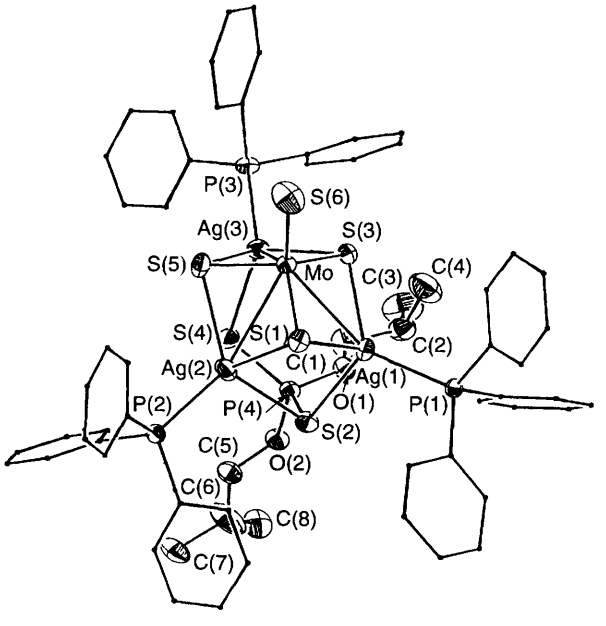


**Fig. 2** Crystal structure of $[MoAg_3S_4(PPh_3)_3\{S_2P(OBu^i)_2\}]$ **2**. Carbon atoms of phenyl rings are presented as dots for clarity

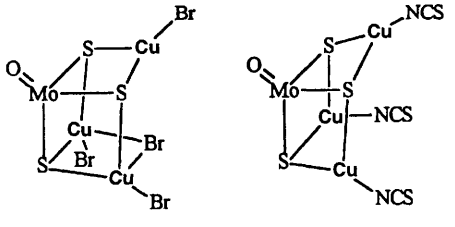


**4** **5**

to the corresponding Cu or Ag atom are always shorter than those of the bidentate S atom to its Cu or Ag atoms. The geometry of the P atom is a distorted tetrahedron. For example, the O–P–O and S–P–S angles are comparable to those found in copper (or silver) dithiophosphate complexes such as $[\{M'(PPh_3)[S_2P(OEt_3)_2]\}_2]$ (M' = Cu or Ag).[13,14]

**Other features of compound 1.** The geometry of $[MoOS_3]^{2-}$ can be described as a distorted tetrahedron with its three Mo–S distances of 2.250(4), 2.261(5), 2.235(5) Å and the Mo–O distance of 1.689(4) Å. This unit acts as a tridentate ligand coordinating to the three Cu atoms through its three $\mu_3$-S atoms. The oxygen atom occupies a terminal position. The average $\mu_3$-S–Cu distance is 2.307(6) Å, similar to those found in a cubane-like cluster $[MoCu_3OS_3(PPh_3)_3Br]$ **3**,[14] a half-open cage-shaped cluster $[MoCu_3OS_3Br_3(\mu\text{-}Br)]^{3-}$ **4**[2c] and a nest-shaped cluster $[MoOS_3\{Cu(NCS)_3\}]^{2-}$ **5**.[15] It is interesting to compare cluster **1** with **3** and **5**. If **3** can be considered as having a closed structure and **5** an open structure, then the skeleton of **1** can be described as intermediate, where the distance S(5)–Cu(1) is much longer than that of a usual S–Cu bond. Some structural parameters of clusters **1**–**5** are listed in Table 4. Considering that the geometry of the $MoOS_3$ unit in **1**, **3** and **5** is nearly identical, a distinction can be made from the Cu–S–Cu and the Cu–Mo–S angles the averages of which decrease from **5** to **3** to **1**.

**Other structural features of compound 2.** The geometry of $[MoS_4]^{2-}$ can also be described as a distorted tetrahedron and comparable to that in $[MoAg_3S_4(PPh_3)_3X]$ (X = Cl, Br or I).[16] Three of the four Mo–S distances in the unit are 2.223(2), 2.223(2) and 2.259(2) Å corresponding to single bonds and the other is 2.029(3) Å falling in the range of a double bond. The average $\mu_3$-S–Ag distance is 2.617(2) Å, slightly longer than 2.558(3) Å in $[MoAg_3S_4(PPh_3)_3Cl]$ **6**[17] or 2.573(3) Å in $[MoAg_3S_4(PPh_3)_3I]$ **7**.[18] The average Mo–Ag distance is 3.043(2) Å, slightly longer than 2.944 Å in **6** or 2.979(2) Å in **7**. Replacement of a halide in the cubane-like cluster by a bulkier dithiophosphate ligand has given rise to an increased solubility in common organic solvents. It has also resulted in certain distortions in the cluster structure. Selected bond lengths and angles of **2**, **6** and **7** are compiled in Table 4 for comparison.

## Optical properties

The electronic spectra of compounds **1** and **2** are displayed in Fig. 3. Peaks (absorption coefficients in dm$^3$ mol$^{-1}$ cm$^{-1}$) occur at 348 ($1.0 \times 10^4$) and 408 nm ($6.4 \times 10^3$) for **1** and 319 ($1.8 \times 10^4$) and 482 nm ($5.9 \times 10^3$) for **2**.

The introduction of the dithiophosphate ligands makes the clusters much more soluble in common organic solvents such as

**Table 2** Selected bond distances (Å) and angles (°) for compound **1**

| | | | | | | | |
|---|---|---|---|---|---|---|---|
| Mo–Cu(1) | 2.772(3) | Cu(1)–S(2) | 2.331(5) | Cu(2)–S(5) | 2.519(6) | S(4)–P(4) | 1.957(7) |
| Mo–Cu(2) | 2.714(3) | Cu(1)–S(3) | 2.301(5) | Cu(2)–P(2) | 2.234(6) | S(5)–P(4) | 2.012(7) |
| Mo–Cu(3) | 2.730(3) | Cu(1)–S(4) | 2.363(6) | Cu(3)–S(1) | 2.318(5) | P(4)–O(1) | 1.579(14) |
| Mo–S(1) | 2.250(4) | Cu(1)–P(1) | 2.304(5) | Cu(3)–S(3) | 2.293(5) | P(4)–O(2) | 1.56(2) |
| Mo–S(2) | 2.261(5) | Cu(2)–S(1) | 2.331(6) | Cu(3)–S(5) | 2.673(6) | O(1)–C(01) | 1.39(3) |
| Mo–S(3) | 2.235(5) | Cu(2)–S(2) | 2.266(5) | Cu(3)–P(3) | 2.224(5) | O(2)–C(05) | 1.39(3) |
| Mo–O | 1.689(14) | | | | | | |
| | | | | | | | |
| Cu(1)–Mo–Cu(2) | 83.60(8) | S(2)–Mo–S(3) | 107.2(2) | S(1)–Cu(2)–S(2) | 104.9(2) | Cu(2)–S(1)–Cu(3) | 87.3(2) |
| Cu(1)–Mo–Cu(3) | 79.78(8) | S(2)–Mo–O | 111.5(5) | S(1)–Cu(2)–S(5) | 92.1(2) | Mo–S(2)–Cu(1) | 74.2(2) |
| Cu(1)–Mo–S(1) | 124.0(2) | S(3)–Mo–O | 112.2(5) | S(1)–Cu(2)–P(2) | 118.0(2) | Mo–S(2)–Cu(2) | 73.6(2) |
| Cu(1)–Mo–S(2) | 54.0(1) | Mo–Cu(1)–S(2) | 51.7(1) | S(2)–Cu(2)–S(5) | 111.4(2) | Cu(1)–S(2)–Cu(2) | 105.4(2) |
| Cu(1)–Mo–S(3) | 53.4(1) | Mo–Cu(2)–S(3) | 51.3(1) | S(2)–Cu(2)–P(2) | 120.7(2) | Mo–S(3)–Cu(1) | 75.3(2) |
| Cu(1)–Mo–O | 124.6(5) | Mo–Cu(2)–S(4) | 129.8(2) | S(5)–Cu(2)–P(2) | 106.0(2) | Mo–S(3)–Cu(3) | 74.2(2) |
| Cu(2)–Mo–Cu(3) | 72.22(9) | Mo–Cu(2)–P(1) | 124.5(2) | Mo–Cu(3)–S(1) | 52.2(1) | Cu(1)–S(3)–Cu(3) | 100.4(2) |
| Cu(2)–Mo–S(1) | 55.1(2) | S(2)–Cu(1)–S(3) | 102.8(2) | Mo–Cu(3)–S(3) | 52.0(1) | Cu(1)–S(4)–P(4) | 108.0(3) |
| Cu(2)–Mo–S(2) | 53.3(1) | S(2)–Cu(1)–S(4) | 120.5(2) | Mo–Cu(3)–S(5) | 99.0(2) | Cu(2)–S(5)–Cu(3) | 76.3(2) |
| Cu(2)–Mo–S(3) | 113.2(1) | S(2)–Cu(1)–P(1) | 110.1(2) | Mo–Cu(3)–P(3) | 151.7(2) | Cu(2)–S(5)–P(4) | 111.0(3) |
| Cu(2)–Mo–O | 134.6(5) | S(3)–Cu(1)–S(4) | 103.2(2) | S(1)–Cu(3)–S(3) | 102.4(2) | Cu(3)–S(5)–P(4) | 112.6(3) |
| Cu(3)–Mo–S(1) | 54.5(1) | S(3)–Cu(1)–P(1) | 115.5(2) | S(1)–Cu(3)–S(5) | 88.5(2) | S(4)–P(4)–S(5) | 116.0(3) |
| Cu(3)–Mo–S(2) | 108.2(1) | S(4)–Cu(1)–P(1) | 105.1(2) | S(1)–Cu(3)–P(3) | 127.7(2) | S(4)–P(4)–O(1) | 109.5(6) |
| Cu(3)–Mo–S(3) | 53.9(1) | Mo–Cu(2)–S(1) | 52.3(1) | S(3)–Cu(3)–S(5) | 116.4(2) | S(4)–P(4)–O(2) | 113.8(7) |
| Cu(3)–Mo–O | 140.3(5) | Mo–Cu(2)–S(2) | 53.1(1) | S(3)–Cu(3)–P(3) | 111.3(2) | S(5)–P(4)–O(1) | 109.0(6) |
| S(1)–Mo–S(2) | 107.8(2) | Mo–Cu(2)–S(5) | 103.4(2) | S(5)–Cu(3)–P(3) | 109.3(2) | S(5)–P(4)–O(2) | 111.5(7) |
| S(1)–Mo–S(3) | 106.5(2) | Mo–Cu(2)–P(2) | 149.5(2) | Mo–S(1)–Cu(2) | 72.6(2) | O(1)–P(4)–O(2) | 94.9(8) |
| S(1)–Mo–O | 111.4(5) | | | Mo–S(1)–Cu(3) | 73.4(1) | | |

**Table 3** Selected bond distances (Å) and angles (°) for compound **2**

| | | | | | | | |
|---|---|---|---|---|---|---|---|
| Ag(1)–Mo | 2.993(2) | Ag(2)–P(2) | 2.430(2) | Ag(3)–S(4) | 2.581(2) | S(2)–P(4) | 1.979(2) |
| Ag(2)–Mo | 3.095(1) | Ag(2)–S(5) | 2.638(2) | Ag(3)–S(5) | 2.602(2) | S(4)–P(4) | 1.974(2) |
| Ag(3)–Mo | 3.041(2) | Ag(2)–S(2) | 2.731(2) | Mo–S(6) | 2.029(3) | P(4)–O(1) | 1.578(4) |
| Ag(1)–P(1) | 2.416(2) | Ag(2)–S(1) | 2.774(2) | Mo–S(5) | 2.223(2) | P(4)–O(2) | 1.589(4) |
| Ag(1)–S(3) | 2.508(2) | Ag(3)–P(3) | 2.435(2) | Mo–S(1) | 2.223(2) | O(1)–C(1) | 1.442(8) |
| Ag(1)–S(1) | 2.622(2) | Ag(3)–S(3) | 2.558(2) | Mo–S(3) | 2.259(2) | O(2)–C(5) | 1.431(6) |
| Ag(1)–S(2) | 2.670(2) | | | | | | |
| | | | | | | | |
| P(1)–Ag(1)–S(3) | 125.94(6) | P(2)–Ag(2)–Mo | 143.40(4) | S(3)–Ag(3)–Mo | 46.61(4) | S(5)–Mo–Ag(3) | 56.72(5) |
| P(1)–Ag(1)–S(1) | 116.28(6) | S(5)–Ag(2)–S(2) | 129.42(6) | S(4)–Ag(3)–S(5) | 95.29(7) | S(5)–Mo–Ag(2) | 56.67(6) |
| P(1)–Ag(1)–S(2) | 108.95(6) | S(5)–Ag(2)–S(1) | 83.15(6) | S(4)–Ag(3)–Mo | 113.03(6) | S(1)–Mo–S(3) | 112.37(7) |
| P(1)–Ag(1)–Mo | 143.66(4) | S(5)–Ag(2)–Mo | 44.76(5) | S(5)–Ag(3)–Mo | 45.58(5) | S(1)–Mo–Ag(1) | 58.14(5) |
| S(3)–Ag(1)–S(1) | 93.08(6) | S(2)–Ag(2)–S(1) | 91.25(6) | S(6)–Mo–S(5) | 104.0(1) | S(1)–Mo–Ag(3) | 129.72(5) |
| S(3)–Ag(1)–S(2) | 111.85(6) | S(2)–Ag(2)–Mo | 100.77(5) | S(6)–Mo–S(1) | 111.4(1) | S(1)–Mo–Ag(2) | 60.27(5) |
| S(3)–Ag(1)–Mo | 47.49(5) | S(1)–Ag(2)–Mo | 44.10(4) | S(6)–Mo–S(3) | 108.88(9) | S(3)–Mo–Ag(1) | 54.92(5) |
| S(1)–Ag(1)–S(2) | 96.07(6) | P(3)–Ag(3)–S(3) | 113.16(6) | S(6)–Mo–Ag(1) | 135.80(9) | S(3)–Mo–Ag(3) | 55.38(5) |
| S(1)–Ag(1)–Mo | 46.07(4) | P(3)–Ag(3)–S(4) | 116.42(6) | S(6)–Mo–Ag(3) | 118.67(9) | S(3)–Mo–Ag(2) | 102.52(5) |
| S(2)–Ag(1)–Mo | 104.89(6) | P(3)–Ag(3)–S(5) | 121.39(6) | S(6)–Mo–Ag(2) | 147.92(8) | Ag(1)–Mo–Ag(3) | 87.22(5) |
| P(2)–Ag(2)–S(5) | 117.45(6) | P(3)–Ag(3)–Mo | 130.05(5) | S(5)–Mo–S(1) | 107.82(7) | Ag(1)–Mo–Ag(2) | 69.39(5) |
| P(2)–Ag(2)–S(2) | 110.45(6) | S(3)–Ag(3)–S(4) | 115.24(6) | S(5)–Mo–S(3) | 112.06(7) | Ag(3)–Mo–Ag(2) | 74.56(4) |
| P(2)–Ag(2)–S(1) | 114.88(6) | S(3)–Ag(3)–S(5) | 92.16(6) | S(5)–Mo–Ag(1) | 120.18(6) | | |

**Table 4** Comparison of bond distances (Å) and angles (°) for $[MoCu_3OS_3(PPh_3)\{S_2P(OBu)_2\}]$ **1**, $[MoAg_3S_4(PPh_3)\{S_2P(OBu^i)_2\}]$ **2**, $[MoCu_3OS_3(PPh_3)_3Br]$ **3**, $[NEt_4]_3[MoCu_3OS_3Br_3(\mu\text{-}Br)]$ **4**, $[MoOS_3\{Cu(NCS)_3\}]^{2-}$ **5**, $[MoAg_3S_4(PPh_3)_3Cl]$ **6** and $[MoAg_3S_4(PPh_3)_3I]$ **7**

| | **1** | **3** | **4** | **5** | **2** | **6** | **7** |
|---|---|---|---|---|---|---|---|
| Mo–S[a] | 2.259(5) | 2.253(7) | 2.260(5) | 2.263(5) | 2.235(2) | 2.248(3) | 2.254(3) |
| Mo–M'[a] | 2.718(3) | 2.707(6) | 2.657(3) | 2.647(5) | 3.043(2) | 2.944(3) | 2.979(2) |
| M'–S[a] | 2.294(5) | 2.277(8) | 2.267(4) | 2.256(5) | 2.617(2) | 2.558(3) | 2.573(3) |
| | | | | | | | |
| M'–S–M' | 87.3(2) | 88.2(2) | 94.6(2) | 98.0(2) | 79.88(6) | 83.3(1) | 82.4(1) |
| | 100.4(2) | 89.0(2) | 100.2(2) | 108.1(2) | 90.35(7) | 89.79(9) | 86.3(1) |
| | 105.4(2) | 91.4(2) | 100.2(2) | 108.7(1) | 110.48(6) | 90.4(1) | 87.3(1) |
| M'–Mo–S[b] | 108.2(1) | 109.2(2) | 115.5(1) | | | | |
| | 113.2(1) | 111.5(2) | 115.5(1) | | | | |
| | 124.0(2) | 112.2(2) | 120.6(2) | | | | |

[a] Average. [b] The S atom is the one across the cubane from M' (Cu or Ag).

dichloromethane, trichloromethane and toluene. For example, the solubility in dichloromethane is in the range $10^{-3}$–$10^{-4}$ mol $dm^{-3}$ whereas related cubane-like clusters $[MM'_3S_4(PPh_3)_3X]$, $[MM'_3S_4X_4]^{3-}$ and half-open cage-shaped clusters $[MM'_3OS_3X_3(\mu\text{-}X)]^{3-}$ (M = Mo or W; M' = Cu or Ag; X = Cl, Br or I) are virtually insoluble ($< 10^{-5}$ mol $dm^{-3}$) in this solvent. The increase in solubility of an inorganic cluster in volatile non-polar solvents could significantly aid studies

**Table 5** Linear and non-linear optical parameters of selected inorganic clusters

| Cluster | Structure | $\lambda_1$/nm | $\varepsilon_1$/dm$^3$ mol$^{-1}$ cm$^{-1}$ | $\lambda_2$/nm | $\varepsilon_2$/dm$^3$ mol$^{-1}$ cm$^{-1}$ | $F_{\frac{1}{2}}$*/J cm$^{-2}$ | $F_5$*/J cm$^{-2}$ | Ref. |
|---|---|---|---|---|---|---|---|---|
| $[MoAg_3S_4BrCl_3]^{3-}$ | Cubic cage | 318 (sh) | $8.9 \times 10^3$ | 473 | $4.6 \times 10^3$ | 0.6 | 0.3 | 1(*a*) |
| $[MoAg_3S_4Br_4]^{3-}$ | Cubic cage | 320 | $9.3 \times 10^3$ | 483 | $4.8 \times 10^3$ | 0.6 | 0.3 | 1(*a*) |
| $[MoAg_3S_4BrI_3]^{3-}$ | Cubic cage | 327 (sh) | $1.8 \times 10^4$ | 491 | $1.2 \times 10^4$ | 0.5 | 0.3 | 1(*a*) |
| $[WAg_3S_4Br_4]^{3-}$ | Cubic cage | 304 | $1.9 \times 10^4$ | 413 | $5.2 \times 10^3$ | 0.7 | 0.5 | 1(*b*) |
| $[WCu_3S_4Br_4]^{3-}$ | Cubic cage | 316 | $1.8 \times 10^4$ | 431 | $6.7 \times 10^3$ | 1.3 | 0.7 | 1(*b*) |
| $[MoCu_3OS_3(NCS)_3]^{2-}$ | Nest | 404 | $3.8 \times 10^3$ | 495 | $9.6 \times 10^2$ | 7 | 2 | 1(*c*) |
| $[MoCu_3OS_3BrCl_2]^{2-}$ | Nest | 408 | $7.3 \times 10^3$ | 500 | $1.7 \times 10^3$ | 10 | 3 | 1(*e*) |
| $[\{MoCu_3OS_3BrI_2\}_2]^{4-}$ | Twin nest | 410 | $1.6 \times 10^4$ | 502 | $4.6 \times 10^3$ | 2 | 0.2 | 1(*d*) |
| $[MoCu_3OS_3(PPh_3)_3\{S_2P(OBu)_2\}]$ | Open cage | 348 | $1.0 \times 10^4$ | 408 | $6.4 \times 10^3$ | 5 | — | This work |
| $[MoAg_3S_4(PPh_3)_3\{S_2P(OBu^i)_2\}]$ | Open cage | 319 | $1.8 \times 10^4$ | 482 | $5.9 \times 10^3$ | 0.8 | 3 | This work |

The NLO properties of the inorganic clusters cited were all measured with excitation laser pulses of 7 ns and 532 nm. * $F_{\frac{1}{2}}$ is defined as the incident fluence needed to reduce the real transmittance through the material to half of the hypothetical transmittance calculated by Beer's law; $F_s$ is the saturation value of the transmitted fluence. Fluence ($F$) is defined as the light energy divided by the area of the light spot.

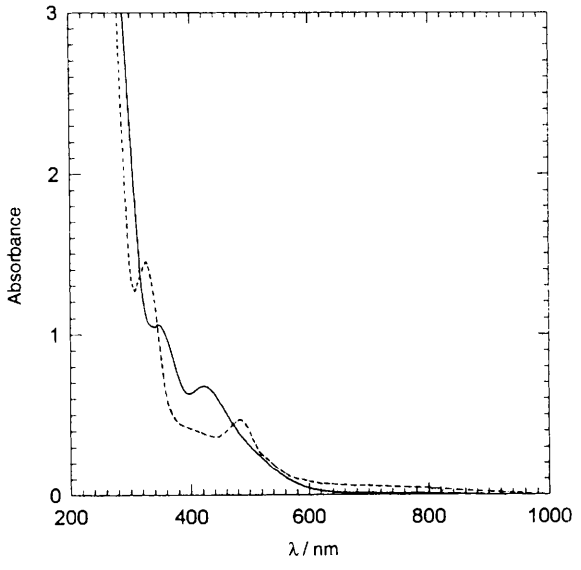


**Fig. 3** Electronic spectra of $[MoCu_3OS_3(PPh_3)_3\{S_2P(OBu)_2\}]$ **1** ($1.04 \times 10^{-4}$ mol dm$^{-3}$, solid curve) and $[MoAg_3S_4(PPh_3)_3\{S_2P(OBu^i)_2\}]$ **2** ($8.1 \times 10^{-4}$ mol dm$^{-3}$, broken curve) in dichloromethane. Optical pathlength 1 mm

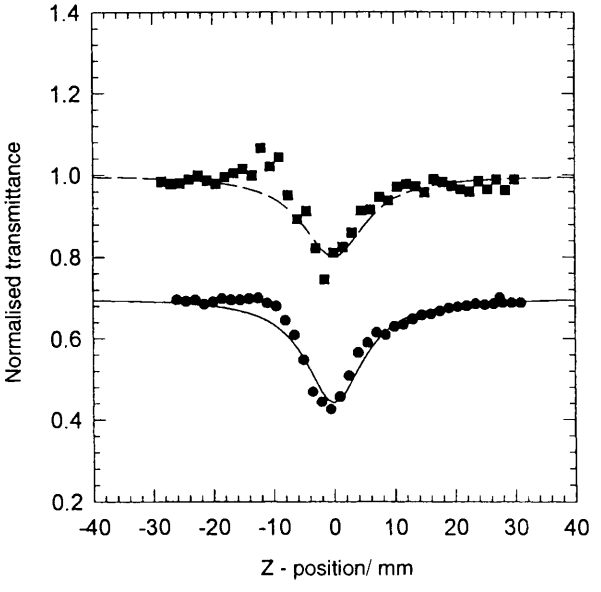


**Fig. 4** Z-Scan data collected in the closed aperture configuration showing the peak–valley data pattern and the self-defocusing effect of $[MoCu_3OS_3(PPh_3)_3\{S_2P(OBu)_2\}]$ **1** (●) and $[MoAg_3S_4(PPh_3)_3\{S_2P(OBu^i)_2\}]$ **2** (■). The aperture diameter was 2.5 cm. The solid and broken curves are based on theoretical calculations in which the self-defocusing effect was set to zero (only NLO absorption is considered)

(currently undertaken in our laboratories) aimed at incorporating them into polymer matrices.

Clusters **1** and **2** have similar NLO properties. Both are self-defocusing and exhibit reverse saturable absorption (RSA)[19] as depicted in Fig. 4. The combination of their NLO refractive property (self-defocusing) and NLO absorptive property (RSA) is in contrast to the behaviour of a regular cubane-like cluster, $[MM'_3S_4X_4]^{3-}$, which typically shows a combination of strong RSA and very weak self-defocusing.[1a,b] Instead, from an NLO point of view, **1** and **2** resemble the half-open cage-shaped clusters.[2c,d] This may not be surprising because the introduction of the dithiophosphate ligands has significantly distorted the skeletal structures of **1** and **2** from that of a regular cubane-like cluster. The Cu(1)–S(5) and Ag(3)–S(2) distances are significantly lengthened as compared to the other Cu–S and Ag–S bond lengths listed in Tables 2 and 3.

From Fig. 4 it is seen that compound **2** exhibits a much stronger self-defocusing effect than does **1**. The stronger the defocusing effects the wider is the spread of transmitted energy. Given the limited size of the detector window (*e.g.* 2.5 cm in this study) and the finite distance from the optical limiting (OL) materials (*i.e.* to the limiter) to the detector, the presence of a strong self-defocusing effect may enhance significantly the overall OL performance of the limiter.

Table 5 lists a few NLO parameters of selected inorganic clusters. From the perspective of OL applications, the incorporation of the bulky dithiophosphate ligands alone will probably neither significantly enhance nor deteriorate the NLO properties of an inorganic cluster. It has been pointed out in our previous papers that the qualitative aspects of the NLO properties of the inorganic clusters studied are dictated by the geometry of their $MM'_3S_3Y$ (Y = S or O) cores. The quantitative aspects are controlled by both the core geometry and the elemental compositions of the cores.[1,2] The completed cubane cores in $[MM'_3S_4(PPh_3)X]$ can more efficiently draw electrons from $PPh_3$ than those in **1** and **2**. Scrutiny of the structure reveals that the cores in regular cubane-like clusters $[MM'_3S_4(PPh_3)X]$, $[MM'_3S_4X_4]^{3-}$ and half-open cage-shaped clusters $[MM'_3OS_3X_3(\mu\text{-}X)]^{3-}$ have much more charge than the cores in **1** and **2**. The relative electron deficiency of the skeletal $MM'_3S_4$ units in **1** and **2** may be responsible for their reduced NLO effect as compared to those of regular cubane-like and half-open cage-shaped clusters.

Within a limited number of series of clusters (such as $[MM'_3S_4X_4]^{3-}$ and the present $[MM'_3S_3Y(PPh_3)_3\{S_2P-$

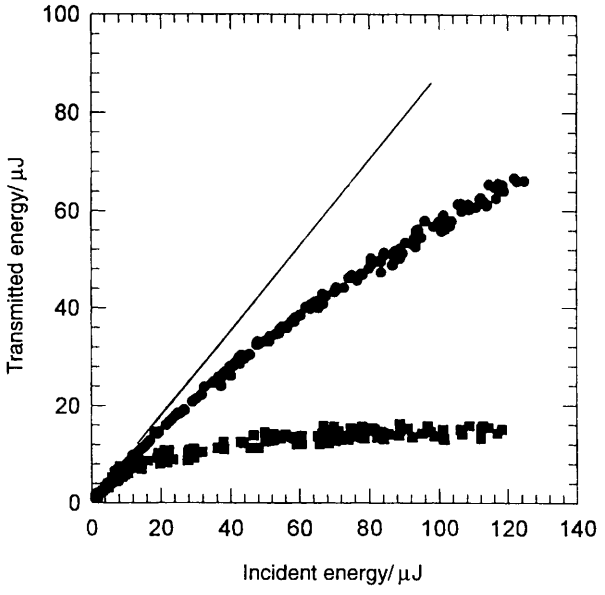


**Fig. 5** Optical limiting effect of $[MoCu_3OS_3(PPh_3)_3\{S_2P(OBu)_2\}]$ **1** ($1.04 \times 10^{-4}$ mol dm$^{-3}$, ●) and $[MoS_4Ag_3(PPh_3)_3\{S_2P(OBu^i)_2\}]$ **2** ($8.1 \times 10^{-4}$ mol dm$^{-3}$, ■). The straight line is an eye guide with 90% transmittance

$(OR)_2\}]$ series) where both the Ag- and the Cu-containing clusters are measured and hence a comparison can be made, the Ag-containing clusters seem always able to outperform their corresponding Cu-containing counterparts in optical limiting at a given wavelength and with similar linear transmittance. The optical limiting ability of **1** and **2** is illustrated in Fig. 5. Under the experimental conditions used, cluster **2** performs much better than **1**. For **2**, the light fluence transmitted starts to deviate from Beer's law when the incident energy ($E_i$) reaches about 12 μJ. Only one half of the incident energy is transmitted when $E_i$ reaches 22 μJ. The transmitted energy clamps effectively at 16 μJ within the energy range studied.

## References


1 (*a*) S. Shi, W. Ji, S. H. Tang, J. P. Lang and X. Q. Xin, *J. Am. Chem. Soc.*, 1994, **116**, 3615; (*b*) S. Shi, W. Ji, J. P. Lang and X. Q. Xin, *J. Phys. Chem.*, 1994, **98**, 3570; (*c*) S. Shi, W. Ji, W. Xie, T. C. Hong, H. C. Zeng, J. P. Lang and X. Q. Xin, *Mater. Chem. Phys.*, 1995, **39**, 298; (*d*) H. W. Hou, X. Q. Xin, J. Liu, M. Q. Chen and S. Shi, *J. Chem. Soc., Dalton Trans.*, 1994, 3211; (*e*) H. W. Hou, X. R. Ye, X. Q. Xin, J. Liu, M. Q. Chen and S. Shi, *Chem. Mater.*, 1995, **7**, 472.

2 (*a*) S. Shi, W. Ji and X. Q. Xin, *J. Phys. Chem.*, 1995, **99**, 894; (*b*) S. Shi, H. W. Hou and X. Q. Xin, *J. Phys. Chem.*, 1995, **99**, 4050; (*c*) S. Shi, Z. R. Chem, H. W. Hou, X. Q. Xin and K. B. Yu, *Chem. Mater.*, 1995, **7**, 1519; (*d*) Z. R. Chem, H. W. Hou, X. Q. Xin, K. B. Yu and S. Shi, *J. Phys. Chem.*, 1995, **99**, 8717; (*e*) G. Sankane, T. Shibahara, H. W. Hou, X. Q. Xin and S. Shi, *Inorg. Chem.*, 1995, **34**, 4785.

3 J. W. McDonald, G. D. Friesen, L. D. Rosenhein and W. E. Newton, *Inorg. Chim. Acta*, 1983, **72**, 205.

4 J.-P. Declercq and M. M. Woolfson, MULTAN 82. A System of Computer Programs for the Automatic Solution of Crystal Structures from X-Ray Diffraction Data, Universities of York and Louvain, 1982.

5 TEXSAN TEXRAY, Structure Analysis Package, Revised, Molecular Structure Corporation, The Woodlands, TX, 1987.

6 D. T. Cromer and J. T. Waber, *International Tables for X-Ray Crystallography*, Kynoch Press, Birmingham: (Present Distributor Kluwer, Dordrecht), 1974, vol. 4, Tables 2.2a and 2.3.1.

7 M. Sheik-Bahae, A. A. Said and E. W. Van Stryland, *Opt. Lett.*, 1989, **14**, 955.

8 M. Sheik-Bahae, A. A. Said, T. H. Wei, D. J. Hagan and E. W. Van Stryland, *IEEE J. Quantum Electron.*, 1990, **26**, 760.

9 (*a*) A. Mueller, U. Schimanski and J. Schimanski, *Inorg. Chim. Acta*, 1983, **76**, L245; (*b*) J. M. Manoli, C. Potvin, F. Secheresse and S. Marzake, *Inorg. Chim. Acta*, 1988, **150**, 257; (*c*) F. Secheresse, S. Bernes, F. Robert and Y. Jeannin, *J. Chem. Soc., Dalton Trans.*, 1991, 2875.

10 S. W. Du and X. T. Wu, *J. Coord. Chem.*, 1993, **30**, 183; *Acta Crystallogr., Sect. C*, 1994, **50**, 500.

11 C. K. Johnson, ORTEP, Report ORNL-5138, Oak Ridge National Laboratory, Oak Ridge, TN, 1976.

12 Q. H. Chen, S. F. Lu and X. Y. Huang, *Chin. J. Struct. Chem.*, 1994, **13**, 102.

13 M. G. B. Drew, R. J. Hobson, P. P. E. M. Mumba and D. A. Rice, *Inorg. Chim. Acta*, 1988, **142**, 301; *J. Chem. Soc., Dalton Trans.*, 1987, 1569.

14 A. Mueller, H. Boegge and U. Schimanski, *Inorg. Chim. Acta*, 1983, **69**, 5.

15 J. P. Lang, S. A. Bao, H. Z. Zhu, X. Q. Xin, J. H. Cai, L. H. En, Y. H. Hu and B. S. Kang, *Gaoden Xuexiao Huaxue Xuebao*, 1992, **13**, 889.

16 A. Mueller, H. Boegge, U. Schimanski, M. Fenk, K. Nieradzik, M. Dartmann, E. Krickemeyer, J. Schimanski, C. Roemer, M. Roemer, H. Dornfield, U. Wienboeker, W. Hellmann and M. Zimmermann, *Monatsh. Chem.*, 1989, **120**, 367; B. C. Shi, F. J. Gao, E. Y. Shao, G. C. Wei and Z. S. Jin, *Chin. J. Struct. Chem.*, 1992, **11**, 225.

17 N. Y. Zhu, J. H. Wu, S. W. Du, X. T. Wu and J. X. Lu, *Inorg. Chim. Acta*, 1992, **191**, 65.

18 J. P. Lang, S. A. Bao, H. Z. Zhu, X. Q. Xin and K. B. Yu, *Chin. J. Chem.*, 1993, **11**, 126.

19 W. Ji, S. Shi, H. J. Du, S. W. Tang and X. Q. Xin, *J. Phys. Chem.*, 1995, **99**, 17297; W. Ji, H. J. Du, S. H. Tang, S. Shi, J. P. Lang and X. Q. Xin, *Sing. J. Phys.*, 1995, **11**, 55.


*Received* 12*th December* 1995; *Paper* 5/08081I